Miscible Viscous Fingering of Pushed versus Pulled Interface

Satyajit Pramanik* and Manoranjan Mishra
Department of Mathematics, Indian Institute of Technology Ropar, Rupnagar – 140001, Punjab, India
*Corresponding author: E-mail: satyajit.math16@gmail.com

Abstract: Viscous fingering (VF) instability has been extensively studied over past several decades in the context of various industrial, environmental and chemical processes. We try to model miscible VF using COMSOL Multiphysics when the interface separating the two fluids is curvilinear, which gives rise to sometimes pushed or pulled interface. We study the effect of the positive and negative log-mobility ratio on the fingering instability. Numerical simulation has been performed in 2D Eulerian frame for different flow parameters such as log-mobility ratio (R), width of the Hele-Shaw cell or porous media (L_y) etc. The dependence of mixing length and number of the fingers on various governing parameters are presented. Grid dependency of the COMSOL Multiphysics simulation for VF instability has been exposed and we propose the optimal grid required for the appropriate simulation, which resembles with various numerical (Fourier-spectral, finite difference methods) results available in literature.

Keywords: Miscible flow, viscous fingering, porous media, pushed and pulled interfaces.

1. Introduction

Miscible VF instability is an interfacial phenomenon, which is observable in flows through porous media with increasing fluid viscosity along the downstream direction [1]. Due to the higher mobility of the displacing fluid it tries to invade the other fluid leading to the deformation of the interface of the fluids. This phenomenon is known as the VF instability [1]. Such instability has significant influence on various fluid flows of commercial interest, such as in chromatographic separation, oil refineries, pollutant contamination in aquifers [2-4], etc. In such situations the displaced fluid is localized within a finite region, which is surrounded by two semi-infinite fluid regions with either same or different physical properties. Depending upon the viscosity jump along the interfaces of the fluids either of the interfaces can become unstable. Extensive theoretical studies [2, 3] of such instability phenomenon and the corresponding COMSL Multiphysics simulation [4] have been successfully conducted in past.

However, all the above-mentioned studies considered ideal situation of flat diffusive fluid interfaces. In realistic situation we may encounter interfaces that can take arbitrary shapes. Maes *et al*. [5] performed a laboratory experiment for displacement of a circular sample by another fluid of lower viscosity in a Hele-Shaw cell. Motivated by the phenomenal results of this experiment we present a COMSOL Multiphysics modeling of miscible VF instabilities of pushed versus pulled interface in this article.

2. Physical description of the problem and its mathematical modeling

Consider a Hele-Shaw cell or a homogeneous porous media filled with an incompressible fluid. Another incompressible fluid has been injected into the system, which is restricted within a circular region. Initially this fluid system is kept stationary. To neglect the effect of gravitational field we assume that the fluids are neutrally buoyant. Viscosity of both the fluids strongly depends upon the solute concentration. The viscosities of the displacing and displaced fluids are taken to be μ_{01} and μ_{02} respectively. Next the fluid with viscosity μ_{01} is continuously supplied from the left of the domain at a uniform speed $u = U_0$. Modeling of this problem has been performed by coupling the Darcy's law with the convection-diffusion equation for the solute concentration. The complete system of governing equations is [1-4],

$$\nabla . \vec{u} = 0 \tag{1}$$

$$\nabla p = -\frac{\mu}{k}\vec{u} \tag{2}$$

$$\frac{\partial c}{\partial t} + \vec{u}.\nabla c = \nabla \cdot (D \nabla c) \tag{3}$$

These equations correspond to various conservation laws. Eq. (1) represents the conservation of mass for incompressible fluids, which is known as the equation of continuity. Eq. (2) is the Darcy's law which determines the two dimensional fluid velocity for pressure driven flow in porous media. The evolution of the solute concentration is characterized by the Eq. (3), which corresponds to the conservation of solute concentration. In the above equations $\vec{u}$ represents the Darcy velocity, μ is the kinematic viscosity of the fluid, p is the dynamic pressure and k corresponds to the permeability of the medium. These equations resemble the Hele-Shaw flow when the small gap width d between the two parallel plates and the permeability of the medium are related by $k = d^2/12$.

The typical relation between the viscosity and the concentration may or may not be an analytic function. However, in our model we consider an Arrhenius relation between them as

$$\mu(c) = \mu_{01} e^{Rc} \qquad (4)$$

Where R is the log-mobility ratio given by

$$R = \ln(\mu_{02}/\mu_{01}) \qquad (5)$$

3. Use of COMSOL Multiphysics

Pramanik *et al.* [4] use COMSOL Multiphysics to model classical miscible VF instability for the displacement of finite fluid confined in a rectangular region in the context of chromatographic columns and aquifers. They have shown that their model is capable of reproducing the results and have very good qualitative agreement with those of Mishra *et al.* [3]. Following the work of Pramanik *et al.* [4] we model the present problem of miscible VF of pushed and pulled interfaces using the CFD module of COMSOL Multiphysics 4.3b. The two-phase Darcy's law (tpdl) model, which combines the time dependent convection-diffusion equation for the solute concentration to the steady Darcy flow equation, has been used. This model consists of two phases of fluids having saturations s_1 and s_2 respectively. The concentration of the fluid is defined as the product of the fluid saturation and its density. Densities of both the phases are taken to be same $\rho = \rho_1 = \rho_2$. The two-phase Darcy's law model of COMSOL Multiphysics eventually becomes identical to the Eqs. (1) – (3) under the assumptions: porosity ε_p, permeability κ, relative permeability $\kappa_{r1} = \kappa_{r2} = 1$, viscosity $\mu = \mu_1 = \mu_2$, in the model equations. The concentration dependent viscosity relation can be expressed in terms of the saturation s_1,

$$\mu = \mu_{01} e^{R s_1} \qquad (6)$$

We perform our simulation in a rectangular domain of dimension $[0, L_x] \times [0, L_y]$. Fluid of viscosity μ_{01} is continuously supplied from the left of the domain at a uniform velocity U_0 to displace the other fluid having viscosity μ_{02}.

Implementation of this model has been carried under the following boundary and initial conditions. Boundary conditions for the fluid velocity are of Dirichlet type at both the inlet and outlet boundaries $x = 0$ and $x = L_x$, whereas concentration takes a constant value at the inlet boundary while it satisfies no flux condition at the outlet boundary. Mathematically we can represent them as: at $x = 0$ $u = U_0$, $s_1 = 0$ and at $x = L_x$ $p = 0$ and $\partial c / \partial x = 0$. Along the transverse boundaries $y = 0$ & $y = L_y$ both velocity and concentration satisfy Neumann type boundary conditions. These boundary conditions specify that fluid neither enters into the domain nor leaves the domain across these boundaries.

An appropriate initial condition for the fluid velocity is linear velocity profile that satisfies the prescribed boundary conditions. The initial saturation of the displaced fluid is taken to be

$$s_1(t=0) = \begin{cases} 1, & (x - x_0)^2 + (y - y_0)^2 \le r^2 \\ 0, & (x - x_0)^2 + (y - y_0)^2 \ge r^2 \end{cases}$$

where (x_0, y_0) and r respectively represent the center and the radius of the circular region where the displaced fluid is confined initially.

The time dependent coupled system is solved using both MUMPS and PARIDOS linear solvers and compared the computational time

taken by each solver. It is verified that for a particular set of flow parameters the computational time taken by one of the solvers can be more or less than the other depending upon the parameter set. A comparison of computational time is presented in Table 1 in the appendix. Hence none of these two solvers has uniformly computational efficiency over other. A user defined "mapped" mesh has been used to discretize the flow domain. Numerical convergence of the solution has been verified by changing the mesh size and all the simulations in this article use extremely fine grids of "fluid dynamics". The parameters used for the simulations in this paper are listed in Table 2.

4. Results and Discussion

Main aim of this present article is to propose an optimal grid modeling of miscible viscous fingering of pushed and pulled interfaces using COMSOL Multiphysics 4.3b and to show the existence of fingering dynamics at such interfaces. Fundamental of hydrodynamic instability is to analyze how a given perturbation to the system evolves with time. Pramanik *et al.* [4] and Holzbecher [6] applied a random noise into the initial condition for the concentration field to trigger the VF instability. Pramanik *et al.* [4] could successfully reproduce the results of Mishra *et al.* [3] qualitatively by keeping the unstable leading or trailing interface initially at the same position in the computational domain. Some of their results are shown in the Fig. 1 (Fig. 1(b)-(c) correspond to the first and third panels of Fig. 1, while Fig. 1(e)-(f) correspond to the first and third panels of Fig. 2 of Pramanik *et al.* [4]) along with the mesh used in the corresponding simulations. However, a suitable explanation of such specific choice of the position of the unstable interface is lacking in their study. We present here the appropriate reasoning behind this with the help of meshing of the computational domain. In their computation a non-uniform free triangular meshing was used. The initial saturation S_1 of the displaced fluid is specified at the vertices of those triangles. Thus although the initial saturation at the interfaces are randomized in the same way as Mishra *et al.* [3], it gets distributed differently at both the interfaces (see Fig. 1(a) and 1(b)). Hence this leads to different fingering patterns (see Fig. 1(c) and 1(d)) for $R > 0$ and $R < 0$. This difficulty was overcome by keeping the respective unstable interfaces at the same initial position (see Fig. 1(c) and 1(f)). Therefore we expect that a uniform meshing can resolve this difficulty to selecting the initial position of the unstable interface.

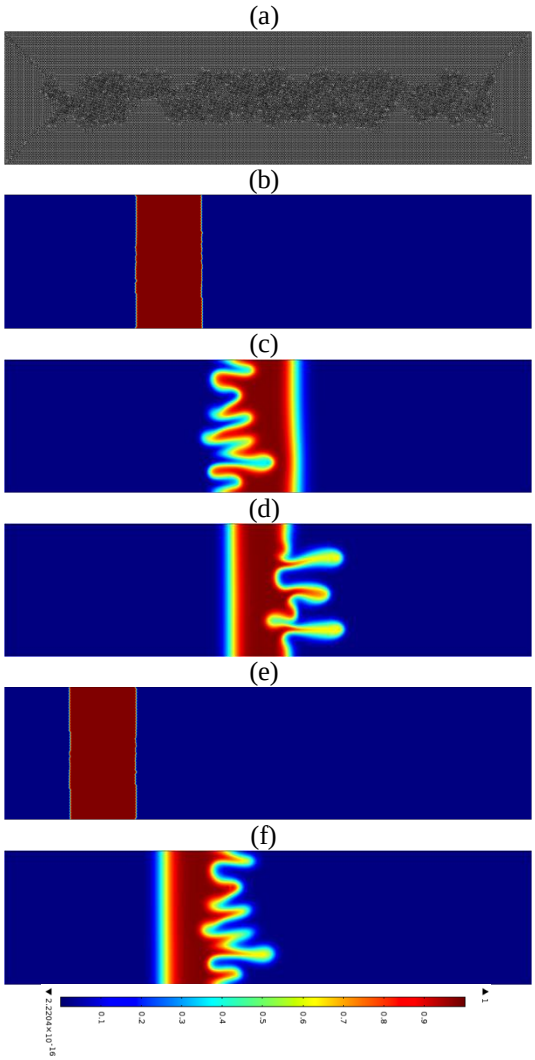

Figure 1. (a) The extra fine free triangular fluid dynamics mesh used by Pramanik *et al.* [4]. (b) - (c) Surface plots of saturation S_1 with $R = 2$ at times t = 0, 10 seconds respectively (Fig. 1 of [4]). (d) Surface plot of saturation S_1 with $R = -2$ at time t = 10 seconds corresponding to the initial saturation distribution as shown in (b). (e) - (f) Surface plots of saturation S_1 with $R = -2$ at times t = 0, 10 seconds respectively (Fig. 2 of [4]). For all the three sets of simulations $U_0 = 1 \times 10^{-3}$ *m/s* and L_y = 0.02 mm.

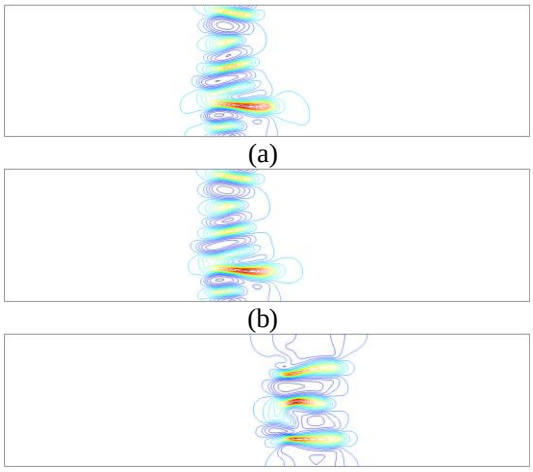

(a)

(b)

(c)

Figure 2. Axial velocity contours at time t = 10 seconds. From top to bottom these correspond to Fig. 1(c), 1(f) and 1(d) respectively.

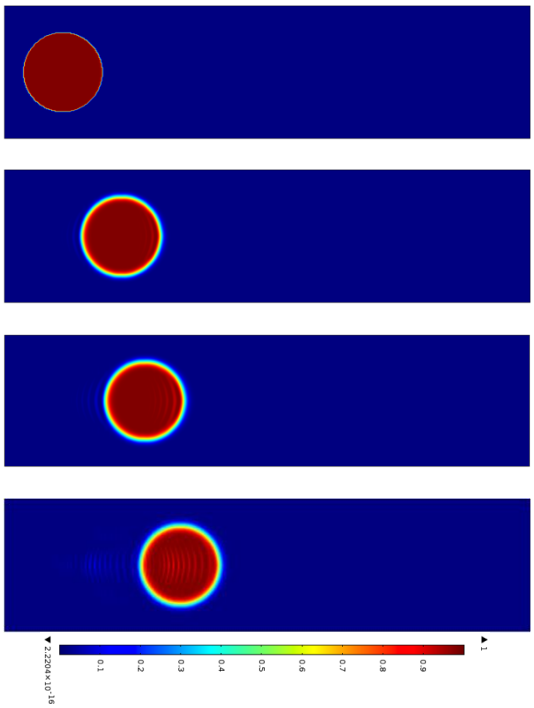

Figure 3. Surface plots of saturation S_1 at successive times showing pure diffusion for $U_0 = 1 \times 10^{-3}$ *m/s*, R = 0, L_y = 0.08 mm. and r = 0.3 × L_y. From top to bottom t = 0, 25, 35, 50 seconds.

In Fig. 2 the axial velocity contours have been plotted at t = 10 for both $R > 0$ and $R < 0$. Fig. 2 (a) - (b) show velocity contours for R = 2 and R = -2 respectively when the respective unstable interfaces are kept at same position (see Fig. 1(b) and 1(e)). The velocity contours for R = -2, associated to the initial saturation distribution represented in Fig. 1(b), are shown in the Fig. 2(c). It clearly depicts that the velocity contours at the unstable interface are same in the first two cases. On the other hand in the third case the velocity contours differ from those of the first two cases. Thus the reproducibility of the results of Mishra *et al.* [3] is possible only if the respective unstable interfaces are kept at the same initial position.

Next, we repeat the same simulation but with mapped meshing, which discretizes the computational domain into squares of uniform size. However, this also does not reproduce the results of Mishra *et al.* [3] qualitatively without changing the initial distribution of the saturation field of fluid. Still this meshing is more preferable over the free triangulation since the randomization of the initial fluid saturation S_1 remains under the user control; it is not redistributed according to the size of the mesh.

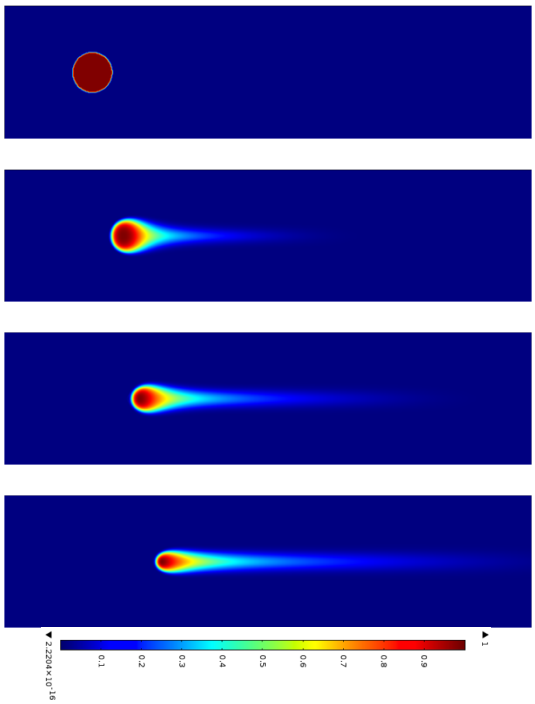

Figure 4. Surface plots of saturation S_1 at successive times showing convective diffusion for $U_0 = 1 \times 10^{-3}$ *m/s*, R = 3, L_y = 0.08 mm. and r = 0.15 × L_y. From top to bottom t = 0, 100, 150, 200 seconds.

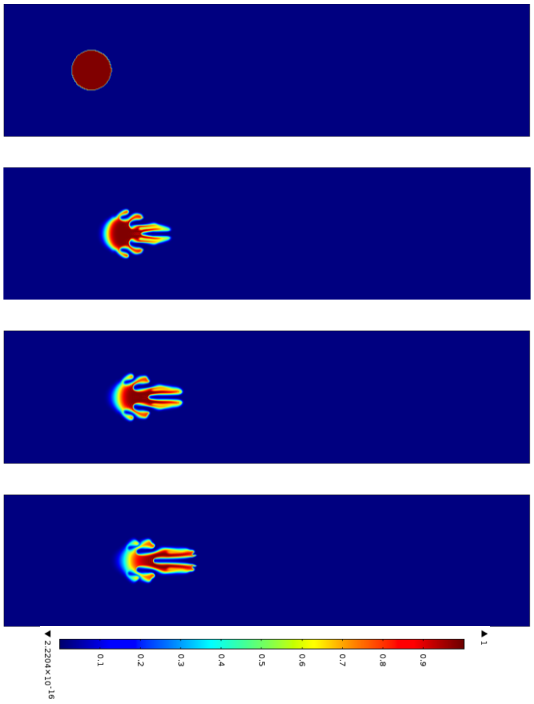

Figure 5. Surface plots of saturation S_1 at successive times with $U_0 = 1 \times 10^{-3}$ *m/s*, $R = -3$, L_y = 0.08 mm. and r = 0.15 × L_y. From top to bottom t = 0, 8, 10, 12 seconds.

Thus we choose the mapped meshing in our consequent simulations for viscous instability at pushed and pulled interfaces. Fig. 3 shows the pure diffusion of one fluid into another both having same viscosity, i.e. when R = 0. In accordance to the classical VF study of single interface fluid displacement, localized circular fluid seems to diffuse out in all directions according to the diffusivity in the longitudinal and transverse directions.

In Fig. 4 the evolution of the saturation field S_1 for R = 3, $U_0 = 1 \times 10^{-3}$ *m/s*, L_y = 0.08 mm. and r = 0.15 × L_y has been represented. From the classical VF instability for the displacement of finite sample it is expected that the fingers will be formed at the backward part of the fluid interface. This part of the interface is pulled in the upstream direction. Hence the VF instability in such case is called VF at pulled interface. However, the expected fingering instability has not been observed at the pulled interface under this circumstance (see Fig. 4). It only endures diffusion accelerated by the convection that helps in the formation of a long tail in the downstream direction. Such a tail formation is already observed in the experiments by Maes *et al.* [5]

Next, we reverse the viscosity contrast between the two fluids i.e. change R = 3 to R = -3 and analyze the pattern formation at the fluid interface. As expected, fingers are observed at the frontal part of the circular fluid, which is pushed in the downstream direction. This is further referred as the VF at pushed interface. Fig. 5 depicts the formation of crown like fingers, which match qualitatively with the results of Chen *et al.* [7] in absence of the Korteweg stresses. Fingers are formed symmetrically about the centerline of the Hele-Shaw cell. This symmetry persists until the nonlinear interaction of the fingers starts. Another important observation is that the trailing half of the circle follows diffusive nature. However, unlike the case of flat interface the shape of the stable diffusive half evolves with time even before the fingers start interacting with it. This is due to the curvilinear nature of the interface.

5. Conclusions and perspectives

We successfully capture the VF dynamics for pulled interface using COMSOL Multiphysics 4.3b. It is observed that the fluid interface does not undergo fingering instability when the viscosity of the displacing fluid is less than the circular one, at least with the parameters used in this article. However, when the surrounding fluid becomes more viscous, fingers are observed. This discrepancy with the traditional finite fluid displacement [3, 4], where both the interfaces lead to fingering instability for any parameters, may be due to the flow velocity through the localized fluid. The influence of log-mobility ratio and the injection speed on the fingering dynamics and all the classical features, such as splitting and merging of fingers remain unchanged under these conditions. However, the dynamics observed in the experiments of Maes *et al.* [5] may be captured by changing various governing parameters such as, increasing circle's radius or reducing the width of the Hele-Shaw cell or the porous media (L_y) etc. Further extensive investigation in this direction is the topic of our ongoing research.

6. References

1. G. M. Homsy, Viscous fingering in porous media, Annu. Rev. Fluid Mech. **19**, 271 (1987).
2. A. De Wit, Y. Bertho, M. Martin, Viscous fingering of miscible slices, *Phys. Fluids* **17**(5), 054114 (2005).
3. M. Mishra, M. Martin, A. De Wit, Differences in miscible viscous fingering of finite width slices with positive or negative log-mobility ratio, *Phys. Review* **E 78**, 066306-(2008).
4. S. Pramanik, G. L. Kulukuru, M. Mishra, Miscible viscous fingering: Application in chromatographic columns and aquifers, COMSOL conference, Bangalore (2012).
5. R. Maes, G. Rousseaux, B. Scheid, M. Mishra, P. Colinet and A. De Wit, Experimental study of dispersion and miscible viscous fingering of initially circular samples in Hele-Shaw cells, *Phys. Fluids* ***22***, 123104 (2010).
6. E. Holzbecher, Modeling of viscous fingering, COMSOL conference, Milan (2009).
7. C. Y. Chen, L. Wang and E. Meiburg, Miscible droplets in a porous medium and the effects of Korteweg stresses, *Phys. Fluids* ***13***, 2447-2456 (2001).

7. Acknowledgements

The financial supports from the Department of the Science and Technology, Govt. of India and the National Board for Higher Mathematics, Govt. of India are gratefully acknowledged.

8. Appendix

Table 1: Comparison of computational time between the linear solvers MUMPS and PARDISO

Parameter set	**Computational time**	
	MUMPS	**PARDISO**
R = -2, L_y = 0.08 mm, r = 0.45× L_y, A = 4	8319 seconds	21345 seconds
R = 2, L_y = 0.08 mm, r = 0.45× L_y, A = 4	2479 seconds	1996 seconds
R = 0, L_y = 0.08 mm, r = 0.3× L_y, A = 4	1912 seconds	466 seconds

Table 2: List of parameters

Parameters	**Symbols**	**Value & Unit**
Length of the domain	L_x	0.32 mm
Width of the domain	L_y	0.08 mm
Log-mobility ratio	R	-3, 0, 3
Injection speed	U_0	1 mm/s
Viscosity of the displacing fluid	μ_{01}	10^{-3} Pa-s
Aspect ratio	A	4
Radius of the circular sample	$r = 0.15\times L_y$ $r = 0.3\times L_y$ $r = 0.45\times L_y$	0.012 mm 0.024 mm 0.036 mm
Center of the circle	$x_0 = L_x/9$, $y_0 = L_y/2$	(0.0356,0.04) (mm)